

Prion Protein Aggregation Induced by Copper(II) and Heparan Sulfate. Pressure-dependent Switch of Reaction Pathways

Driss El Moustaine, Joan Torrent, and Reinhard Lange

Univ Montpellier 2, Montpellier, F-34095 France; Inserm, U710, Montpellier, F-34095 France; EPHE, Paris, F-75007 France

Reprint requests to Reinhard Lange. E-mail: reinhard.lange@inserm.fr

Z. Naturforsch. **2008**, *63b*, 747–755; received March 4, 2008

Dedicated to Professor Gérard Demazeau on the occasion of his 65th birthday

Copper ions (Cu^{2+}) and heparan sulfate (HS) are suspected to act as regulatory agents in the conversion of cellular prion protein (PrP^{C}) to its infectious isoform. However, the mechanism of this reaction is still largely unknown. Our previous report suggested multidimensional pathways for structural alterations of PrP, which may be modulated by high pressure (HP). Here we use HP to investigate the effects of Cu^{2+} and HS binding on PrP conformational changes and assembly. In the presence of Cu^{2+} , amyloid fibrils are formed only under HP. In contrast, in the presence of HS, fibrils are formed at atmospheric pressure, but not under HP. Both compounds appear to compete for the same binding site, since HS-supported fibril formation is quenched by Cu^{2+} . Inversely, Cu^{2+} -mediated fibril formation under HP is inhibited by HS.

Key words: Prion Protein, Copper, Heparan Sulfate, Amyloid Fibrils, High Pressure

Introduction

Transmissible Spongiform Encephalopathies (TSEs, or prion diseases) are characterized by a structural change from cellular prion protein (PrP^{C}) to its abnormal and pathological form (PrP^{Sc}). The latter is isolated from TSE infected brain tissue [1]. Whereas PrP^{C} is an α -helical soluble monomer, which is sensitive to proteinase K, PK-insensitive PrP^{Sc} is largely made up of β -sheets and adopts an amyloid fibrillar quaternary structure [2]. It is yet unknown whether TSE infectivity is transmitted by PrP^{Sc} or by an oligomeric or amyloid precursor structure [3–6].

Many reports have shown that the conversion from soluble α -helical to amyloid fibrillar proteins can be induced under protein structure destabilizing conditions. Since then, tremendous efforts have been undertaken to partly unfold prion proteins by means

of elevated temperature, moderate concentrations of chaotropic compounds, or mechanical treatment, in order to reproduce *in vitro* the PrP^{C} to PrP^{Sc} conversion [7–11]. Legname and co-workers [12] succeeded in transforming PrP^{C} to an amyloid PrP^{Sc} -like structure, capable of transmitting TSE in a particular strain of transgenic mice. However, it seems now that the success of this method is restrained to these mice, as the application in other animal models has not been reported. As a consequence, other physico-chemical perturbation methods are sought to further investigate the PrP structure conversion reaction.

For some years now, HP has been used as an alternative prion structure perturbing tool [13–16]. The advantage of pressure is that it specifically perturbs weak van der Waals and electrostatic interactions by favoring the hydration of hydrophobic and charged residues. The origin of these effects is the decreased volume of the hydrated protein compared to the sum of non-hydrated protein plus bulk water. Stacking of aromatic residues is promoted under HP, whereas formation and breaking of hydrogen bonds is relatively pressure insensitive [17, 18]. Pressure appears thus as a powerful tool for inducing the conversion of an α -helical protein to its amyloid fibril structure, since such a reac-

The abbreviations used are: PrP: prion protein; PrP^{C} : cellular isoform; PrP^{Sc} : pathogenic isoform; mPrP^{23–230}: murine full-length recombinant prion protein; HP: high pressure; HS: heparan sulfate; TEM: transmission electron microscopy; ANS: 8-anilino-1-naphthalene sulfonate; ThT: thioflavine T; FTIR: Fourier transform infrared; IR: infrared.

tion requires opening (hydration) of the native globular structure and intermolecular stacking of β -sheets, *i. e.*, two reaction steps which are favored by pressure. As a result, pressure has been shown to promote the formation of PrP amyloid fibrils *via* several intermediate states [19–21]. However, this reaction was found to depend strongly on other physico-chemical parameters. For example, at alkaline pH, incubation at HP leads to spherical PrP particles of about 20 nm in diameter, whereas HP-incubation at neutral pH and in the presence of small amounts of chaotropic compounds results in amyloid fibrils [22].

Another difficulty in the investigation of the PrP^C to PrP^{Sc} conversion is the role of co-factors. Very early in the history of prion research, additional compounds, termed co-factors, or “compound X” have been suspected to take part in this reaction [23,24]. Among the many proposed compounds, copper ions (Cu^{2+}) and sulfated glycosaminoglycans (or heparan sulfate, HS) appear particularly promising. Both compounds have been shown to interact with native PrP^C [25–31]. However, their respective role remains unclear. Some reports suggest that they promote [29–32], and others that they inhibit [33,34] the structural conversion of PrP. Here we used HP as a structure perturbation tool to investigate the structural effects of Cu^{2+} and HS binding on murine full-length recombinant PrP (mPrP^{23–230}). We address the question why under certain conditions these compounds act as inhibitory or as activating co-factors of the conversion from PrP^C to its amyloid fibril structures.

Results

Effects of Cu^{2+} and HP on amyloid formation

Aggregation process

At pH = 7.4 and at 37 °C, and in the absence of chaotropic compounds, PrP stayed soluble under atmospheric pressure as well as under HP, even after several days of incubation. However, in the presence of 1 mM CuCl_2 , the protein aggregated within 2 d, both under HP and atmospheric pressure. The aggregation process is illustrated for the HP condition in Fig. 1. The sigmoidal shape of the time-dependent light scattering intensity shows a two-phase aggregation mechanism: a 24 h lag-time, consisting probably of a nucleation reaction, is followed by massive protein aggregation. After decompression, the aggregates stayed in suspension (they did not sediment).

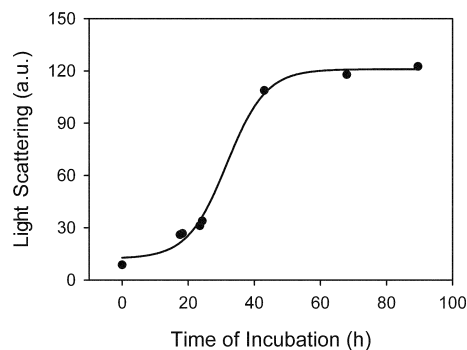


Fig. 1. Aggregation of mPrP^{23–230} at HP (600 MPa) in the presence of 1 mM CuCl_2 . The aggregation was followed by the intensity of light scattering at 340 nm as a function of time. Solution conditions: protein at 2 mg/mL in Tris HCl 20 mM buffer, pH = 7.4 at 37 °C.

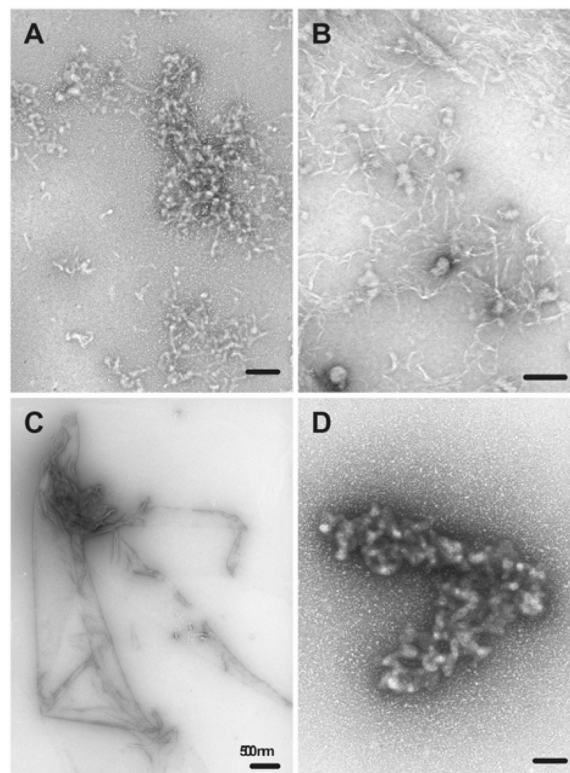


Fig. 2. Negatively stained TEM micrographs of mPrP^{23–230} aggregates formed after 3 days incubation at atmospheric pressure (A and C) and 600 MPa (B and D) in the presence of 1 mM CuCl_2 (A and B) or 20 $\mu\text{g mL}^{-1}$ HS (C and D).

Macrostructure

Incubation in the presence of Cu^{2+} at atmospheric pressure and HP led to two different types of aggregates. As shown in Fig. 2, the aggregates formed at at-

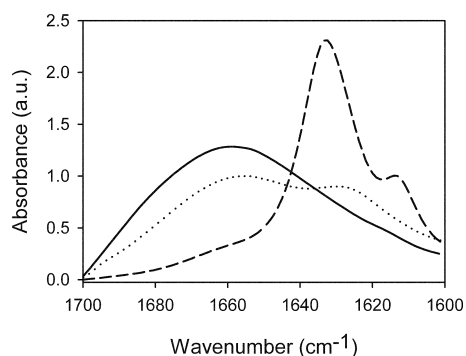


Fig. 3. FTIR spectra of aggregates formed after 3 days incubation in the presence of Cu^{2+} . Cu-amorphous aggregates, formed at atmospheric pressure (dotted line), and Cu-fibrils, formed at HP (dashed line), are compared to the native protein structure (solid line). The spectra were energy-normalized. The incubation conditions were those of Fig. 1.

atmospheric pressure were amorphous (Fig. 2A). In contrast, the aggregates formed after incubation under HP had fibrillar character (Fig. 2B). The diameter of the fibrils was shown to be about 10 nm. Below, the two types of aggregates will be termed Cu-amorphous aggregates and Cu-fibrils.

Secondary structure

The secondary structures of the Cu-amorphous aggregates and Cu-fibrils were analyzed by recording their FTIR amide I band. As shown in Fig. 3, the soluble native protein was characterized by a broad asymmetric absorption band, centered at 1656 cm^{-1} , indicative of a predominantly α -helical structure. This is in good agreement with the reported PrP^C structure obtained from NMR studies [35]. The Cu-amorphous aggregates were characterized by an only slight decrease of the α -helix band, concomitant with a small increase of the β -sheet content. In contrast, the spectrum of the Cu-fibrils showed an intense sharp band at 1630 cm^{-1} , characteristic of a β -sheet structure. In addition, the FTIR spectrum of the Cu-fibrils showed a minor band at 1613 cm^{-1} , which can be attributed to intermolecular β -sheet hydrogen bonding [36].

Tertiary and quaternary structure

Aniline-8-naphthalene sulfonate (ANS) was used to estimate the degree of unfolding of PrP fibrils and amorphous aggregates. Upon partial protein unfolding, ANS binds to water-exposed large hydrophobic protein domains. Its binding results in a large increase of

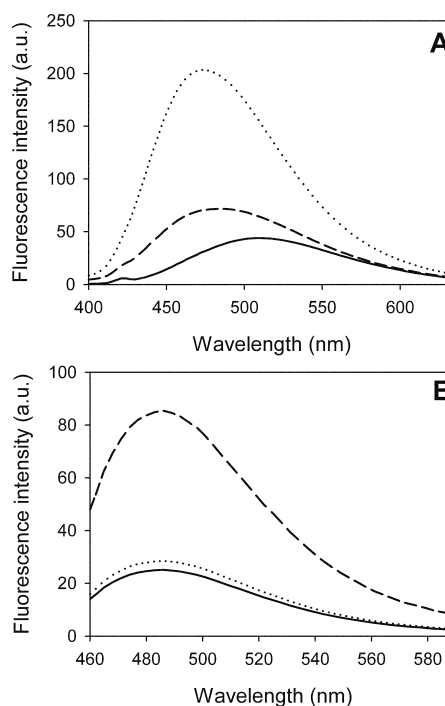


Fig. 4. Fluorescence emission spectra of ANS (A) and ThT (B) of aggregates formed in the presence of 1 mM CuCl_2 at atmospheric pressure and HP: Cu-amorphous aggregates (dotted line) and Cu-fibrils (dashed line). For comparison, the native protein is shown as a solid line. The incubation conditions were those of Fig. 1. For fluorescence measurements, aliquots of soluble and aggregated PrP (2 mg mL^{-1}) were diluted 29 times with 50 mM Tris-HCl , $\text{pH} = 8.5$, and incubated with either $10\text{ }\mu\text{M ThT}$ for 1 min or $50\text{ }\mu\text{M ANS}$ for 10 min at r. t. before monitoring fluorescence.

fluorescence when compared to the emission of free ANS in aqueous solution. Fig. 4A shows that ANS has bound strongly to Cu-amorphous aggregates. Accordingly, the Cu-amorphous aggregates appear to consist of partially unfolded protein. In contrast, the Cu-fibrils exhibited only weak binding to ANS. This indicates that either these aggregates were not made up of partially unfolded proteins, or the ANS binding sites were occluded due to intermolecular collapse of hydrophobic domains in large highly structured aggregates.

The interaction of Thioflavin T (ThT) with the crossed- β -pleated sheet protein structure is common to a variety of oligomers and specifically to amyloid fibrils [37,38]. As shown in Fig. 4B, ThT fluorescence was strongly increased in the presence of PrP Cu-fibrils. In contrast, the fluorescence intensity of Cu-amorphous aggregates was very similar to that of native PrP.

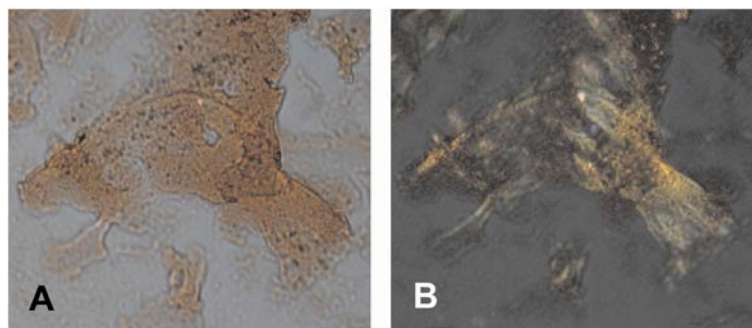


Fig. 5. Birefringence of polarized light after Congo-red staining of pressure-induced PrP Cu-fibrils in the presence of 1 mM CuCl₂: (A) under bright field and (B) under polarized light.

Congo-red staining was used to further characterize the amyloid nature of the aggregates. This dye is believed to interact with the β -sheet structure of amyloids by a molecular alignment in a very regular manner, resulting in a characteristic green birefringence. Consistent with the presence of amyloid-like structures, Cu-fibrils showed green birefringence when viewed under polarized light (Fig. 5).

Effects of HS and HP on amyloid formation

Macrostructure of aggregates

Upon addition of 20 $\mu\text{g/mL}$ HS, PrP aggregated immediately. At atmospheric pressure the aggregates remained as a stable suspension in buffer for up to 3 d. However, at HP they sedimented on the bottom of the cuvette and formed a big cluster. The macrostructure of these aggregates was assessed by transmission electron microscopy (TEM), as shown in Figs. 2C and 2D. Incubation for 3 d at atmospheric pressure led to PrP fibrils. In contrast, incubating the protein for the same time interval at HP (600 MPa) resulted in amorphous aggregates. Below, the two types of aggregates will be termed HS-amorphous aggregates and HS-fibrils. The effect of HS was therefore the opposite of that of Cu²⁺. In the presence of Cu²⁺, fibrils were formed under HP and amorphous aggregates under atmospheric pressure.

Secondary structure

The secondary structures of HS-amorphous aggregates and HS-fibrils, formed after incubation with HS at HP and atmospheric pressure, respectively, were analyzed by their FTIR amide I band (Fig. 6). The HS-amorphous aggregates were characterized by a moderate decrease of their α -helix band, concomitant with a moderate increase of the β -sheet content. However,

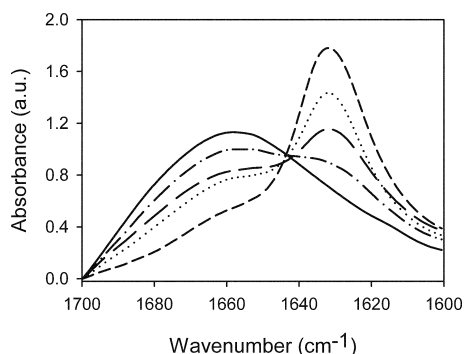


Fig. 6. FTIR spectra of aggregates formed after 3 days incubation in the presence of 20 $\mu\text{g mL}^{-1}$ HS at atmospheric pressure and HP: HS-fibrils, formed at atmospheric pressure (short dashed line), and HS-amorphous aggregates, generated at HP (600 MPa) (long dashed line). Incubation in the presence of both co-factors together, Cu²⁺ and HS, yielded amorphous aggregates at atmospheric pressure (dashed and dotted line) and oligomeric structures at HP (dotted line). The native protein is presented as a solid line.

the spectrum of HS-fibrils showed a strong, sharp band at 1630 cm^{-1} and a strongly decreased intensity at 1656 cm^{-1} , indicative of greatly enhanced β -sheet content, at the expense of the α -helix structure.

Tertiary and quaternary structure

Similarly to the experiments in the presence of Cu²⁺, the aggregates formed in the presence of HS were assessed for their capacity of binding ANS and ThT. As shown in Fig. 7A, HS-fibrils strongly bind ANS, indicating the exposure of large hydrophobic domains of a partly unfolded protein. In contrast, HS-amorphous aggregates showed only a weak fluorescence increase. Again, it should be recalled that opposite ANS binding properties were observed with Cu²⁺-induced aggregates: Cu-amorphous aggregates showed strong and Cu-fibrils only very weak ANS binding,

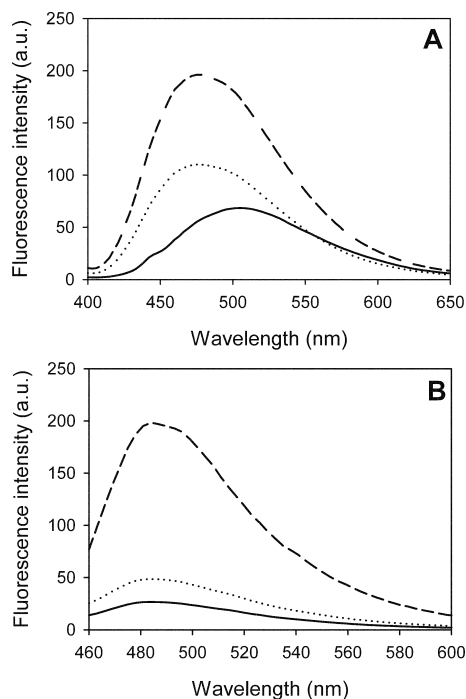


Fig. 7. Fluorescence emission spectra of ANS (A) and ThT (B) of aggregates formed after 3 days incubation in the presence of $20 \mu\text{g mL}^{-1}$ HS at atmospheric and at HP. HS-amorphous aggregates were formed at HP (dots) and HS-fibrils at atmospheric pressure (dashes). For comparison, the native protein is shown as a solid line. The experimental conditions were those of Fig. 4.

cf. Fig. 4A. This suggests that the tertiary structure of amorphous aggregates and fibrils depends on whether they are formed in the presence of Cu^{2+} or HS. The quaternary structure of the aggregates seems, however, not to depend on the nature of the co-factors. This is illustrated in Fig. 7B, reflecting the binding of HS-induced aggregates with ThT. HS-fibrils showed a strong and HS-amorphous aggregates a weak interaction with this fluorophore. A very similar result was observed for Cu^{2+} -induced aggregates (*cf.* Fig. 4B).

Competition of Cu^{2+} and HS for binding to $m\text{PrP}^{23-230}$

Previous studies have shown that Cu^{2+} and HS interact with the *N*-terminal domain of PrP. Their respective binding sites are shown in Fig. 8. In order to investigate whether this competition interferes with the conversion of PrP to amyloid fibrils, PrP was incubated in the presence of both 1 mM CuCl_2 and $20 \mu\text{g mL}^{-1}$ HS for 3 d at atmospheric pressure or under HP (600 MPa).

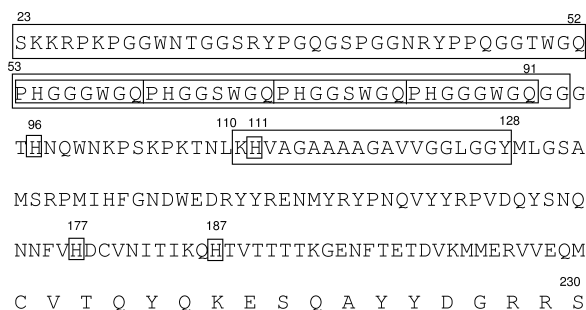


Fig. 8. Amino acid sequence of $m\text{PrP}^{23-230}$ showing the binding sites of Cu^{2+} and HS. The binding sites of HS are shown as boxes, and the binding sites of Cu^{2+} as boxes with amino acids marked in bold.

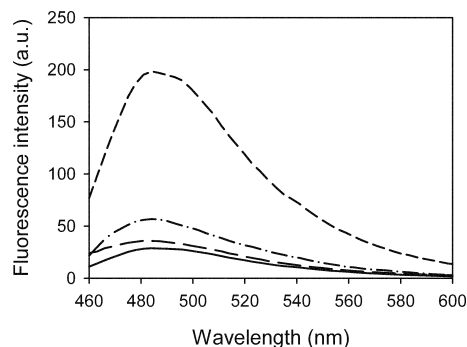


Fig. 9. Effect of the presence of both Cu^{2+} and HS on the ThT fluorescence intensity. $m\text{PrP}^{23-230}$ was incubated 3 days in the presence of 1 mM CuCl_2 and $20 \mu\text{g mL}^{-1}$ HS at atmospheric pressure (long dashes) or HP (600 MPa, dashes plus dots). The solid line shows the spectrum in the presence of the native protein, and the short dashed line the spectrum in the presence of HS-fibrils (obtained in the presence of HS in the absence of Cu^{2+}).

The morphology of the generated aggregates was assessed by TEM (results not shown). In the presence of both co-factors, no fibrils were formed, regardless of the incubation pressure.

The effects of incubation in the presence of both co-factors together on protein secondary structural features were then investigated by FTIR. As shown in Fig. 6, the aggregates formed at atmospheric pressure were rather similar to the native structure, with only a small decrease of the α -helix content, concomitant with a small increase of the β -sheet structure. In contrast, after incubation under HP, the β -sheet content rose significantly, although not to the extent of that of HS-fibrils. A similar behavior was observed when ThT binding was assessed. As shown in Fig. 9, incubation under HP in the presence of both Cu^{2+} and HS increased the fluorescence due to ThT binding, without

attaining the intensity observed with HS-fibrils, suggesting some oligomeric quaternary structure. In contrast, the tertiary structure, assessed *via* ANS binding, was not affected by pressure (results not shown).

Discussion

The possible dependence on co-factors, such as Cu^{2+} or HS, of the PrP^{C} to PrP^{Sc} conversion is of increasing importance in recent prion research. Two questions are generally addressed: i) does the structural conversion of PrP require the presence of a co-factor, and, if yes, by which mechanism does the co-factor interact? ii) Would it be possible to block this structural conversion by the presence of a co-factor, binding to PrP^{C} ? The conflicting literature data on the binding effects of Cu^{2+} and HS to PrP prompted us to investigate different scenarios by which these compounds cause PrP conformational changes.

Copper ions

Under atmospheric pressure binding of Cu^{2+} resulted in a partial unfolding of PrP, without major changes of its secondary structure. Only a slightly increased β -sheet character at the expense of the α -helix was observed. No sign of an ordered oligomeric structure was detected, and the protein formed amorphous aggregates. Although it is evident that Cu^{2+} affects the conformation of PrP, there are several differing views about the structural effects of Cu^{2+} -binding to PrP. Our results are in line with previous reports about Cu^{2+} -dependent PrP aggregation with enhanced β -sheet structure [39] or with proteinase-K resistance [32]. Formation of amorphous aggregates is also consistent with the work of Baskakov and co-workers who found that Cu^{2+} inhibits the formation of amyloid fibrils by stabilizing a nonamyloidogenic PK-resistant form of PrP [40]. In fact, multiple Cu^{2+} binding sites have been identified. They are all within the unstructured *N*-terminal part of the protein. The strongest ones are situated in the octapeptide repeat region [41], which, depending upon the species, comprises 4–5 tandem repeats of the sequence PHGGGW-GQ. Other binding sites are situated close to the amino acid residues His 96 and His 111. At maximum copper occupancy, PrP can bind up to six Cu^{2+} , each coordinated by a single His imidazole group and two deprotonated backbone amide nitrogen atoms [42, 43]. In this coordination mode, each of the octapeptide repeats, as well as His96 and His111 bind a single Cu^{2+} .

In contrast, Cu^{2+} binding under HP induced a very different structural conversion. The secondary structure of the protein changed radically from an α -helix to a β -sheet. The protein polymerized then to form well ordered amyloid fibrils, as attested by ThT fluorescence, electron microscopy and Congo-red birefringence. The pressure dependence of the copper effects may be explained in two ways. Under HP, either the protein- Cu^{2+} interaction mechanism is different, or Cu^{2+} binds to different sites than at atmospheric pressure. Support for the first possibility comes from recent reports showing that Cu^{2+} is capable of binding by different mechanisms, leading to either intramolecular or intermolecular binding to adjacent sites [44, 45]. Indeed, under conditions of low copper occupancy, single Cu^{2+} ions can bind simultaneously to two His. This explains the tendency of PrP-Cu^{2+} to form oligomers as a consequence of Cu^{2+} coordination to His residues from more than one PrP molecule. By privileging the intermolecular pathway, pressure may thus favor the pathway leading to ordered fibrils.

Heparan sulfate

In striking contrast to the effects of Cu^{2+} , incubation of PrP with HS led to amyloid fibrils at atmospheric pressure. A well described effect of PrP interaction with sulfated glycans is the formation of oligomeric polydisperse complexes with decreased solubility properties, and a strong perturbation of its *N*-terminal domain structure [46]. Depending on glycosaminoglycan concentration, a time dependent aggregation was observed, which has been attributed to the reduction in the α -helical content of PrP [47]. Our results are also consistent with the work of Wong *et al.* (2001), who showed that sulfated glycans induce a conformational change in PrP that stimulates the formation of a proteinase-K resistant isoform. The binding sites of HS have been identified as the domain spanning residues 23 and 52, the octa-repeat region, and the domain between residues 110 and 128. These three sites present independent binding affinities toward HS, the strongest one being the PrP octa-repeat region.

Interestingly, the fibril formation did not take place under HP, and amorphous aggregates were formed instead. Their spectral and structural characteristics resembled those of amorphous aggregates, which precede the formation of PrP spherical particles under HP in the absence of HS [22]. This suggests that pressure

prevents, at least to some extent, the interaction of the protein with HS. Indeed, HS bears several negatively charged sulfate groups, and their interaction with positively charged protein residues can be expected to be weakened under HP, due to electrostriction [48]. Another explanation that we cannot rule out is that even if the interaction takes place, the HP treatment hinders the subsequent conformational rearrangement leading to fibrils.

The inhibition of the formation of HS-induced fibrils at atmospheric pressure by Cu^{2+} suggests a competition of Cu^{2+} and HS for a common binding site. This is also supported by the work of Warner *et al.* [49], revealing a Cu^{2+} -induced weakening of the interaction of PrP^C with HS. Common binding sites are the four octa-repeats and the domain between residues 110 and 128. Besides a competition between Cu^{2+} and HS toward a common binding site, PrP interaction with Cu^{2+} might also induce a modified protein conformation in which the HS binding site is occluded.

Nevertheless, at HP, the binding of Cu^{2+} to PrP is not sufficient to prevent completely the HS interaction. The findings in this study support an HS effect on PrP at HP, even in the presence of Cu^{2+} . Our observation that the Cu^{2+} -HP treatment induced a PrP conformational transition to a β -sheet-rich form with fibrillar character, and the fact that the addition of HS results in amorphous aggregates containing some oligomeric ordering as indicated by an increase in ThT fluorescence, corroborate that the Cu^{2+} -induced inhibition of PrP-HS interaction is incomplete at HP.

Thermodynamic versus kinetic control of fibril formation

To resume, Cu^{2+} and HS may be considered as co-factors inducing either amorphous protein aggregation or amyloid fibril formation. HP favors fibril formation in the presence of Cu^{2+} , and amorphous aggregation in the presence of HS. In the presence of both co-factors together, amorphous aggregates are formed, regardless of the pressure. Previous results obtained in the absence of co-factors indicated that amyloid fibrils are the thermodynamically more stable state, whereas amorphous aggregation is kinetically favored [22]. In the case of prion proteins, fibril formation is very slow. It can occur only under conditions where the more rapid amorphous aggregation is strongly slowed down. For example, in the absence of co-factors, at alkaline pH, rapid protein unfolding leads to amorphous ag-

gregates, whereas fibrils are formed only after several days of incubation under HP at neutral pH in the presence of chaotropic agents at very low concentration [22]. A similar thermodynamic/kinetic control may play a decisive role in the presence of co-factors. Fibrils can be formed only under conditions where the protein is not quickly assembled. This would be the case in the presence of Cu^{2+} under HP, and in the presence of HS at atmospheric pressure. All other conditions lead to rapid protein assembly followed by the formation of amorphous aggregates.

Obviously, PrP structural conversions are occurring within a complex energy landscape, offering multiple reaction pathways. Perhaps only one of them leads to the infectious structure. This pathway has not yet been identified. Given the long incubation period of prion diseases, one may expect that it is an extremely slow pathway, *i. e.*, it occurs under conditions where alternative routes, such as amorphous aggregations are prevented (or slowed down). In order to prevent fibril formation, it is therefore reasonable to search for co-factors accelerating the formation of non-toxic amorphous aggregates. For this purpose, the many possible structure conversion pathways should be further explored. For that, HP now appears as a powerful tool, as it permits to populate reaction intermediates which can escape detection under atmospheric pressure [21].

Materials and Methods

Protein expression and purification

The gene encoding mPrP^{23–230} was cloned into pET22b(+) vector (Invitrogen) and expressed in *Escherichia coli* BL21(DE3) after IPTG induction. Recombinant PrP accumulated as inclusion bodies. After lysis, sonication and solubilization of the inclusion bodies by GdnHCl, purification of PrP was performed essentially as described by Rezaei and co-workers [50], using a Ni sepharose column. Refolding of the protein was achieved on the column by heterogeneous phase renaturation simultaneously to purification. The purified protein was recovered in the desired buffer by elution on a G25 desalting column. Final protein concentration was measured by the optical density at 280 nm using an extinction coefficient value of $63495 \text{ cm}^{-1} \text{ mol}^{-1}$, deduced from the composition of the protein. Protein purity and homogeneity were verified by SDS-PAGE and immunoblotting, as well as reversed-phase HPLC using a 214TP10415 C4 column (Vydac). The purified protein was found to be of

the expected molecular weight by ES/MS (electrospray mass spectrometry) on a VG Bio-Q quadrupole with a mass range of 4000 Da (Bio-Tech). Proteins were stored lyophilized.

Structural characterization at HP

For HP experiments, the protein was dissolved in 20 mM Tris-HCl buffer at pH = 7.4. This buffer was selected for its relatively low pH-dependence on pressure. The final protein concentration was 2 mg mL⁻¹, and experiments were performed at 37 °C. CuCl₂ and HS were used respectively at 1 mM and 20 μg/mL. Protein aggregation was followed by monitoring the changes in light scattering intensity at 340 nm (4 nm slit widths) using an Aminco-Bowmann Series 2 luminescence spectrometer (SLM Aminco) modified to accommodate a thermostated pressure cell. Following each pressure change, typically in steps of 40 MPa, the sample was allowed to equilibrate for 10 min before the next measurement.

Transmission electron microscopy (TEM)

The aggregates obtained by pressurization were diluted to 0.5 g L⁻¹, deposited onto carbon-coated grids and negatively stained with freshly filtrated 2% uranyl acetate, dried, and then viewed in a JOEL 1200EX² electron microscope at an accelerating voltage of 80 kV.

ThT and ANS binding

Fluorescence measurements were performed at 20 °C with a FluoroMax-2 fluorimeter (Jobin Yvon-Spex) with a 10 × 4 mm path length rectangular cuvette. Aliquots of soluble and aggregated PrP (2 mg mL⁻¹) were diluted 29 times with 50 mM Tris HCl, pH = 8.5, and incubated with either 10 μM ThT for 1 min or 50 μM ANS for 10 min at r. t. before monitoring fluorescence. For ANS spectra, excitation was at 385 nm (4 nm slit). Each emission spectrum (4 nm slit) was the average of three scans. ThT emission spectra were recorded after excitation at 450 nm (excitation

slit was 4 nm; emission slit was 4 nm), with each spectrum being the average of three scans. Contributions due to scattered light were subtracted from the signal as follows: a protein sample spectrum in the absence of the corresponding fluorescent probe was collected at each pressure so that contributions from light scattering could be subtracted.

FTIR spectroscopy

The infrared spectra were obtained with a Bruker Vertex 80v FTIR spectrometer equipped with a liquid nitrogen cooled broad band MCT solid-state detector. The spectra (256 scans accumulation) were co-added after registration at a spectral resolution of 2 cm⁻¹ and analyzed by the OPUS 6.0 program. For comparison of soluble and aggregated protein, all spectra were recorded with dry samples. Comparison of dried protein and samples in solution did not reveal significant changes in their FTIR spectra. After isolation of aggregates by centrifugation (8500 g for 2 min), and suspension in buffer, the sample was deposited onto a CaF₂ plate, where the solvent was allowed to evaporate overnight at r. t. To compare qualitatively the spectra of different samples, we normalized each spectrum with respect to the integrated intensity of the entire spectrum.

Congo-red staining and birefringence

An aggregated protein suspension was air-dried on a glass microscope slide. The sample was stained by using the Congo-red kit from Sigma (Aldrich). Birefringence was observed with a Leica DM IRM light microscope (Leica Microsystems SA) equipped with polarizers.

Acknowledgements

This work was carried out in the frame of the European COST Chemistry D30. It was supported by the European grant NEUROPRION and by PPF 2007-2010 to C. Picart. The authors thank Th. Crouzier for technical help with the Vertex 70 FTIR apparatus.

-
- [1] S. B. Prusiner, *Science* **1982**, *216*, 136–144.
 [2] S. B. Prusiner, *Science* **1997**, *278*, 245–251.
 [3] B. Caughey, P. T. Lansbury, *Ann. Rev. Neurosci.* **2003**, *26*, 267–298.
 [4] R. Chiesa, D. A. Harris, *Neurobiol. Dis.* **2001**, *8*, 743–763.
 [5] J. Kazlauskaitė, A. Young, C. E. Gardner, J. V. Macpherson, C. Venien-Bryan, T. J. Pinheiro, *Biochem. Biophys. Res. Commun.* **2005**, *328*, 292–305.
 [6] S. Simoneau, H. Rezaei, N. Sales, G. Kaiser-Schulz, M. Lefebvre-Roque, C. Vidal, J. G. Fournier, J. Comte, F. Wopfner, J. Grosclaude, H. Schatzl, C. I. Lasmezas, *PLoS Pathog.* **2007**, *3*, 1175–1186.
 [7] H. Rezaei, Y. Coiset, F. Eghiaian, E. Treguer, P. Men-

- tre, P. Debeye, J. Grosclaude, T. Haertle, *J. Mol. Biol.* **2002**, 322, 799–814.
- [8] G.S. Jackson, L.L. Hosszu, A. Power, A.F. Hill, J. Kenney, H. Saibil, C.J. Craven, J.P. Waltho, A.R. Clarke, J. Collinge, *Science* **1999**, 283, 1935–1937.
- [9] W. Swietnicki, M. Morillas, S.G. Chen, P. Gambetti, W.K. Surewicz, *Biochemistry* **2000**, 39, 424–431.
- [10] K.W. Leffers, J. Schell, K. Jansen, R. Lucassen, T. Kaimann, L. Nagel-Steger, J. Tatzelt, D. Riesner, *J. Mol. Biol.* **2004**, 344, 839–853.
- [11] K.W. Leffers, H. Wille, J. Stohr, E. Junger, S.B. Prusiner, D. Riesner, *Biol. Chem.* **2005**, 386, 569–580.
- [12] G. Legname, I.V. Baskakov, H.O. Nguyen, D. Riesner, F.E. Cohen, S.J. DeArmond, S.B. Prusiner, *Science* **2004**, 305, 673–676.
- [13] J. Torrent, M.T. Alvarez-Martinez, F. Heitz, J.P. Liautard, C. Balny, R. Lange, *Biochemistry* **2003**, 42, 1318–1325.
- [14] J. Torrent, M.T. Alvarez-Martinez, M.C. Harricane, F. Heitz, J.P. Liautard, C. Balny, R. Lange, *Biochemistry* **2004**, 43, 7162–7170.
- [15] J. Torrent, M.T. Alvarez-Martinez, J.P. Liautard, C. Balny, R. Lange, *Protein Sci.* **2005**, textit14, 956–967.
- [16] Y. Cordeiro, J. Kraineva, R. Ravindra, L.M. Lima, M.P. Gomes, D. Foguel, R. Winter, J.L. Silva, *J. Biol. Chem.* **2004**, 279, 32354–32359.
- [17] V.V. Mozhaev, K. Heremans, J. Frank, P. Masson, C. Balny, *Proteins* **1996**, 24, 81–91.
- [18] C.A. Royer, *Biochim. Biophys. Acta* **2002**, 1595, 201–209.
- [19] Y.S. Kim, T.W. Randolph, M.B. Seefeldt, J.F. Carpenter, *Methods Enzymol.* **2006**, 413, 237–253.
- [20] J. Torrent, C. Balny, R. Lange, *Protein Pept. Lett.* **2006**, 13, 271–277.
- [21] J. Torrent, M.T. Alvarez-Martinez, J.P. Liautard, R. Lange, *Biochim. Biophys. Acta* **2006**, 1764, 546–551.
- [22] D. El Moustaine, V. Perrier, L. Smeller, R. Lange, J. Torrent, *FEBS J.* **2008**, 275, 2021–2031.
- [23] C. Fasano, V. Campana, C. Zurzolo, *J. Mol. Neurosci.* **2006**, 29, 195–214.
- [24] S. Supattapone, *J. Mol. Med.* **2004**, 82, 348–356.
- [25] B. Caughey, G.J. Raymond, *J. Virol.* **1993**, 67, 643–650.
- [26] R. Gabizon, Z. Meiner, M. Halimi, S.A. Ben-Sasson, *J. Cell. Physiol.* **1993**, 157, 319–325.
- [27] B. Caughey, K. Brown, G.J. Raymond, G.E. Katzenstein, W. Thresher, *J. Virol.* **1994**, 68, 2135–2141.
- [28] D.R. Brown, K. Qin, J.W. Herms, J.W. Madlung, A.J. Manson, R. Strome, P.E. Fraser, T. Kruck, A. von Bohlen, W. Schulz-Schaeffer, A. Giese, D. Westaway, H. Kretzschmar, *Nature* **1997**, 390, 684–687.
- [29] C. Wong, L.W. Yiong, M. Horiuchi, L. Raymond, K. Wehrly, B. Chesebro, B. Caughey, *EMBO J.* **2001**, 20, 377–386.
- [30] D. McKenzie, J. Bartz, J. Mirwald, D. Olander, R. Marsh, J. Aiken, *J. Biol. Chem.* **1998**, 273, 25545–25547.
- [31] G.M. Shaked, Z. Meiner, I. Avraham, A. Taraboulos, R. Gabizon, *J. Biol. Chem.* **2001**, 276, 14324–14328.
- [32] K. Qin, D.S. Yang, Y. Yang, M.A. Chishti, L.H. Meng, H.A. Kretzschmar, C.M. Yip, P.E. Fraser, D. Westaway, *J. Biol. Chem.* **2000**, 275, 19121–19131.
- [33] M. Perez, F. Wandosell, C. Colaco, J. Avila, *Biochem. J.* **1998**, 335 (Pt 2), 369–374.
- [34] N. Hijazi, Y. Shaked, H. Rosenmann, T. Ben-Hur, R. Gabizon, *Brain Res.* **2003**, 993, 192–200.
- [35] R. Riek, S. Hornemann, G. Wider, R. Glockshuber, K. Wüthrich, *FEBS Lett.* **1997**, 413, 282–288.
- [36] G. Zandomenighi, M.R. Krebs, M.G. McCammon, M. Fandrich, *Protein Sci.* **2004**, 13, 3314–3321.
- [37] H. LeVine, 3rd, *Protein Sci.* **1993**, 2, 404–410.
- [38] R. Carrotta, R. Bauer, R. Waninge, C. Rischel, *Protein Sci.* **2001**, 10, 1312–1318.
- [39] J. Stockel, J. Safar, A.C. Wallace, F.E. Cohen, S.B. Prusiner, *Biochemistry* **1998**, 37, 7185–7193.
- [40] O.V. Bocharova, L. Breydo, V.V. Salmikov, I.V. Baskakov, *Biochemistry* **2005**, 44, 6776–6787.
- [41] M.P. Hornshaw, J.R. McDermott, J.M. Candy, J.H. Lakey, *Biochem. Biophys. Res. Commun.* **1995**, 214, 993–999.
- [42] C.S. Burns, E. Aronoff-Spencer, C.M. Dunham, P. Lario, N.I. Avdievich, W.E. Antholine, M.M. Olmstead, A. Vrieling, G.J. Gerfen, J. Peisach, W.G. Scott, G.I. Millhauser, *Biochemistry* **2002**, 41, 3991–4001.
- [43] C.E. Jones, M. Klewpatinond, S.R. Abdelraheim, D.R. Brown, J.H. Viles, *J. Mol. Biol.* **2005**, 346, 1393–1407.
- [44] M. Chattopadhyay, E.D. Walter, D.J. Newell, P.J. Jackson, E. Aronoff-Spencer, J. Peisach, G.J. Gerfen, B. Bennett, W.E. Antholine, G.L. Millhauser, *J. Am. Chem. Soc.* **2005**, 127, 12647–12656.
- [45] M.A. Wells, C. Jelinska, L.L. Hosszu, C.J. Craven, A.R. Clarke, J. Collinge, J.P. Waltho, G.S. Jackson, *Biochem. J.* **2006**, 400, 501–510.
- [46] R. Gonzalez-Iglesias, M.A. Pajares, C. Ocal, J.C. Espinosa, B. Oesch, M. Gasset, *J. Mol. Biol.* **2002**, 319, 527–540.
- [47] O. Andrievskaia, Z. Potetinova, A. Balachandran, K. Nielsen, *Arch. Biochem. Biophys.* **2007**, 460, 10–16.
- [48] E. Nicolai, A. Di Venere, N. Rosato, A. Rossi, A. Finazzi Agro, G. Mai, *FEBS J.* **2006**, 273, 5194–5204.
- [49] R.G. Warner, C. Hundt, S. Weiss, J.E. Turnbull, *J. Biol. Chem.* **2002**, 277, 18421–18430.
- [50] H. Rezaei, D. Marc, Y. Choiset, M. Takahashi, G. Hui Bon Hoa, T. Haertle, J. Grosclaude, P. Debey, *Eur. J. Biochem.* **2000**, 267, 2833–2839.